# Barrier Structure for Ga-Free Type-II Superlattice Midwave Infrared Photodetector

P. Christol[1], M. Bouschet[1,2], J. P. Perez[1] and N. Péré-Laperne[2]
[1]*IES, Univ. Montpellier, CNRS, Montpellier, France*
[2]*LYNRED, BP 21, Veurey-Voroize, France*

Keywords: Midwave Infrared Photodetector, Barrier Structure, Ga-Free Type-II Superlattice.

Abstract: This paper reports on electrical and electro-optical characterizations of Ga-free InAs/InAsSb type-II superlattices (T2SL) midwave infrared barrier photodetectors grown by Molecular Beam Epitaxy on GaSb substrate. Experimental measurements are made of photo-response and dark current density-voltage (J-V) measurements performed as a function of temperature and transport of minority carrier in this barrier detector is discussed. Results obtained at 150 K for 5µm cut-off wavelength are at the state of the art but identification of an high bias voltage operation demonstrates that the barrier layer has to be improved.

## 1 INTRODUCTION

High performance cooled photodetectors operating in the midwave infrared (MWIR, 3-5µm) atmospheric spectral window are used in a wide variety of applications in imaging and sensing. To keep high signal to noise ratio, it is necessary to reduce the operating temperature of the IR detector system to cryogenic temperatures, which involves the implementation of a cryocooler inducing significant restrictions in term of weight, compactness and energy autonomy. Mitigating these constraints is essential to generate new class of applications using, for example, handheld thermal imagers or embedded systems on unmanned aerial vehicles. Consequently, enhancing the temperature operation, without penalizing performance of detectors, is currently one of the main challenges investigated by the IR detector community.

InSb (Indium Antimonide) and MCT (Mercury Cadmium Telluride) cooled photodetectors are the currently dominant technologies in the MWIR domain. However, despite high performances reached, such commercial technologies have some limits : InSb suffers from a low Shockley-Read-Hall lifetime, close to 700 ns, limiting its operating temperature at 80-90K ; MCT can operate at temperature as high as 110-120K for 5µm cut-off but is very challenging to manufacture and a few number of providers can handle it. Consequently, there is a need to develop an new MWIR technology with high temperature operation (T = 150 K) and strain-balanced Ga-free InAs/InAsSb Type-II superlattice (T2SL) on GaSb substrate, especially combined with a barrier structure design, seems promising to address some of these limitations.

Since the work reported by Maimon and Wicks (Maimon and Wicks, 2006) on InAs detector, barrier structure also called XBn (Klipstein, 2011), is now the usual design of high performance MWIR photodetector. In a barrier structure, a large band gap material, namely the barrier layer (BL), is inserted after the absorption layer (AL) to block the majority carriers while allowing unimpeded transport of the minority carriers to the contact layer (CL). The electric field being confined in the BL, the generation-recombination (G-R) current is suppressed in the absorption region and the dark-current of such a structure, when properly designed, is thus diffusion-limited whatever the temperature. The electrical performances of XBn devices are therefore improved compared to the usual pin photodiodes and temperature operation as high as 150 K is reached for the MWIR (Ting, 2018), but many works have still to be done to improve their electrical and electro-optical performances.

This paper reports on design, fabrication and characterization of Ga-free InAs/InAsSb T2SL MWIR photodetector, grown by molecular beam epitaxy (MBE) on GaSb substrate.



Christol, P., Bouschet, M., Perez, J. and Péré-Laperne, N.
Barrier Structure for Ga-Free Type-II Superlattice Midwave Infrared Photodetector.
DOI: 10.5220/0011624500003408
In *Proceedings of the 11th International Conference on Photonics, Optics and Laser Technology (PHOTOPTICS 2023)*, pages 21-27
ISBN: 978-989-758-632-3; ISSN: 2184-4364

## 2 DESIGN OF THE GA-FREE INAS/INASSB SUPERLATTICE BARIER STRUCTURE

The three semiconductor materials InAs, GaSb, and AlSb form an approximately lattice-matched set around 6.1 A, covering a wide range of band-gap energies (Figure 1).

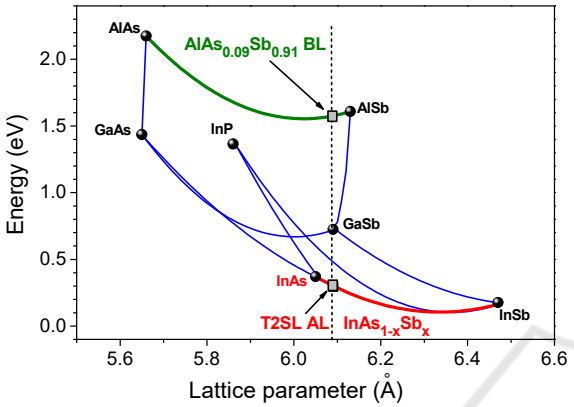


Figure 1: Band-gap energy as a function of lattice parameter of common III-V semiconductor materials. The dashed line shows the lattice parameter of GaSb compound near 6.1 A.

Considering a GaSb substrate, Ga-free InAs/$InAs_{1-x}Sb_x$ T2SLs can be strain-balanced on GaSb by choosing appropriate combinations of layer thicknesses and $InAs_{1-x}Sb_x$ alloy compositions. Typically, the tensile strain in InAs is compensated by the compressive strain introduced in $InAs_{1-x}Sb_x$ leading to a thicker InAs layer compared to the InAsSb one. Precisely, strain balancing is achieved by setting the average lattice parameter of one period of the SL equal to the lattice parameter of GaSb. Consequently, the InAsSb and InAs layer thicknesses ($t_{InAsSb}$ and $t_{InAs}$, respectively) as a function of the Sb composition ($x_{Sb}$) and T2SL period (P) can be calculated by using the equations :

$$t_{InAsSb} = \left(\frac{a_{GaSb} - a_{InAs}}{a_{InSb} - a_{InAs}}\right).\left(\frac{P}{x_{Sb}}\right) = 0.090\,.\left(\frac{P}{x_{Sb}}\right) \quad (1)$$

$$t_{InAs} + t_{InAsSb} = P$$

with $a_{GaSb}$ =6.0954 Å ; $a_{InAs}$ = 6.0584 Å ; $a_{InSb}$ =6.4794 Å, the lattice parameters of the binary compounds.

Figure 2 shows the evolutions of $t_{InAsSb}$ and $t_{InAs}$ as a functions of antimony concentration ($x_{Sb}$) for a 6nm period thick of strain-balanced InAs/$InA_{1-x}Sb_x$ T2SL. For a given $x_{Sb}$ value, one can extract the thicknesses of each SL layer.

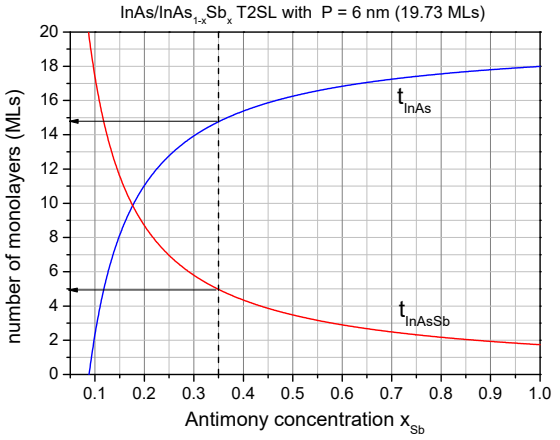


Figure 2: Calculated InAs and InAsSb thicknesses as functions of $x_{Sb}$ for a 6nm (19.73 monolayer (MLs)) period of strain-balanced InAs/InAsSb T2SL on GaSb substrate. Considering an $InAs/InAs_{0.65}Sb_{0.35}$ SL structure, strain-balanced condition is obtained for $t_{InAs}$ = 14.7 MLs and $t_{InAsSb}$ = 5 MLs.

The quantized miniband energies of the strain balanced $InAs/InAs_{1-x}Sb_x$ T2SL, for different antimony concentrations $x_{Sb}$ and SL period, were calculated using the **k p** formalism and the envelope function approximation available in the Nextnano3 commercial software.

A type II-b InAs/InAsSb heterostructure band offset, with electrons confined in the InAs layer and holes confined in the InAsSb one, has been taken into account (Lakner, 2012 ; Steenbergen, 2012). Due to this band alignment, inducing a spatial indirect valence to conduction energetic transition, the absorption coefficient of the InAs/InAsSb T2SL has a strong dependence on the electron-hole wavefunction overlap $|\langle\Phi_C|\Phi_V\rangle|^2$ which is governed by the $x_{Sb}$ composition and period thickness of the strain-balanced SL (Webster, 2015).

Results in terms of cut-off wavelength of expected Ga-free MWIR T2SL detector system corresponding to the ground heavy hole VH1 to conduction C1 interminiband absorption, are plotted on Figure 3. Calculations were made at T = 150K for $x_{Sb}$ composition varying from 0.25 to 0.4 and T2SL period (P) varying from 4 nm to 8 nm. $|\langle\Phi_{C1}|\Phi_{VH1}\rangle|^2$ wavefunction overlap values calculated for each fundamental VH1-C1 transition are specified. We can note that the wavefunction overlap can be increased by shortening the period of the superlattice for a given Sb concentration, or decreasing the Sb concentration for a given period P.

In order to reach the full MWIR spectral band with cut-off wavelength equal to 5µm, $InAs/InAs_{1-x}Sb_x$ SL structure with Sb content

$x_{Sb}$ = 0.35 and SL period p = 6nm made of $t_{InAs}$=4.5 nm (14.7 MLs) and $t_{InAs}$=1.5 nm (5MLs) could be of interest since this T2SL exhibits cut-off wavelength higher than 5 µm at 150K for a wavefunction overlap higher than 50% (Figure 3).

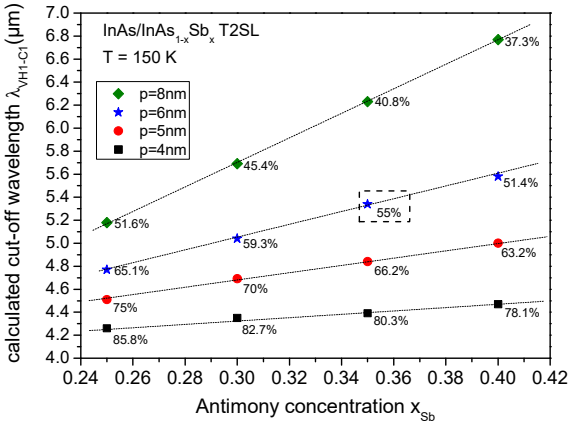


Figure 3: Strain balanced InAs/$InAs_{1-x}Sb_x$ T2SL on GaSb substrate: Calculated cut-off wavelength at T = 150K and associated wavefunction overlap of the ground VH1-C1 miniband transition as a function of Sb concentration ($x_{Sb}$) and for different period thicknesses (P).

Figure 4 displays the schematic band diagram of the chosen InAs(4.5nm)/$InAs_{0.65}Sb_{0.35}$(1.5nm) T2SL structure at T= 150K, showing a fundamental $|\langle\Phi_{C1}|\Phi_{VH1}\rangle|^2$ wavefunction overlap equal to 55%.

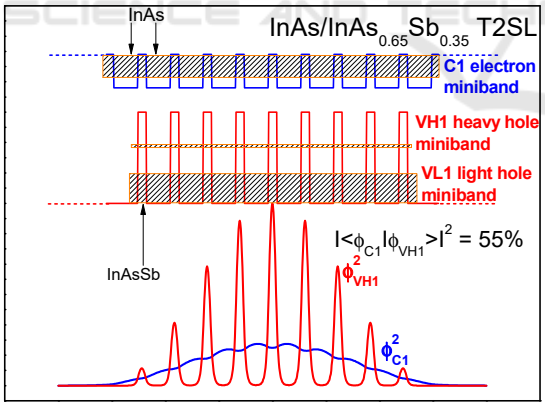


Figure 4: Schematic band diagram of the Ga-free InAs/$InAs_{0.65}Sb_{0.35}$ T2SL structure. On the lower part, fundamental electron (C1) and heavy hole (VH1) presence probability densities are reported, showing a wavefunction overlap equal to 55%.

Dedicated structures have been grown by molecular beam epitaxy (MBE) on GaSb substrate to perform absorption measurement (Arounassalame, 2022). Figure 5 shows the absorption coefficient for temperature ranging from 90 K to 300 K. At λ = 3.4 µm, the absorption coefficient α reaches 4800 $cm^{-1}$ at 150 K. At these temperature, Figure 6 displays the calculated absorption for different absorbing layer thicknesses. For an InAs/InAsSb T2SL layer thickness equal to 3µm, the absorption value at λ = 3.4 µm is over 80%.

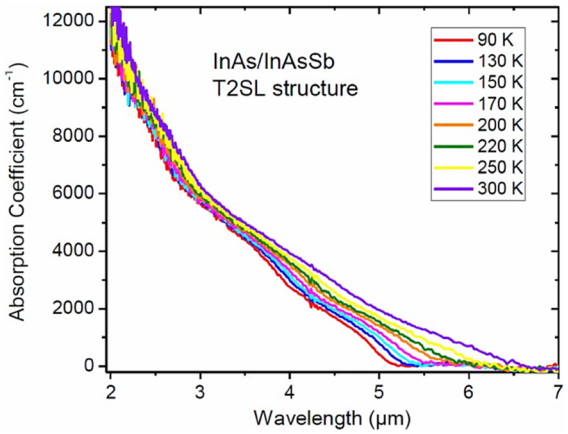


Figure 5: Absorption coefficient versus wavelength of InAs (4.5 nm) /$InAs_{0.65}Sb_{0.35}$ (1.5 nm) T2SL at various temperatures.

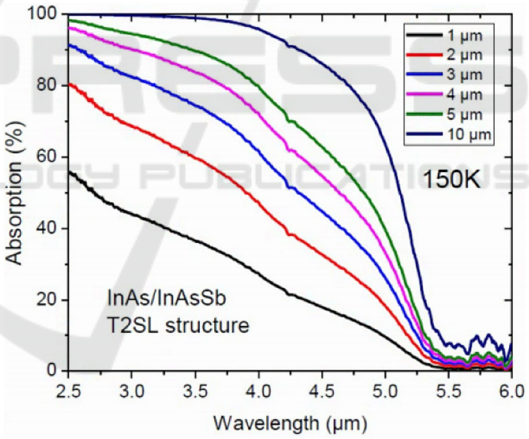


Figure 6: Absorption value versus wavelength of InAs (4.5 nm) /$InAs_{0.65}Sb_{0.35}$ (1.5 nm) T2SL with different layer thicknesses.

Such n-type 3µm-thick T2SL structure is the AL of the XBn detector structure. A adequate BL has to be chosen to block the electron majority carriers. The high band-gap energy of $AlAs_{0.09}Sb_{0.91}$ lattice-matched to the GaSb substrate (Figure 1) could be a good candidate as BL. Furthermore, AlSb/InAs heterostructure presents a staggered type-II band alignment which should not impede the transport of hole minority carriers to the CL (Kroemer, 2004).

## 3 FABRICATION OF THE Ga-Free BARRIER DETECTOR

The Ga-free InAs/InAsSb XBn T2SL detector structure, presented in Figure 7, was epitaxially grown on 2-inch n-type (Te-doped) GaSb (100) substrate by MBE using a 412 RIBER machine.

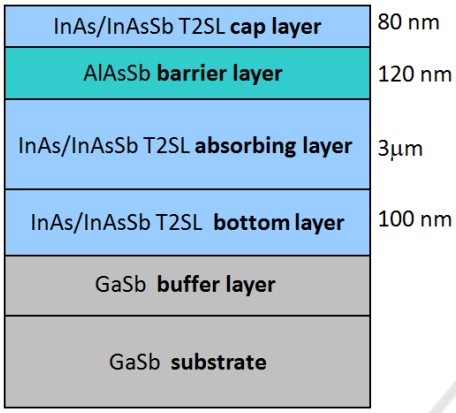


Figure 7: XBn detector structure : Schematic view of the different epilayers stacking on GaSb substrate.

The detector structure consists, from top to bottom, of 80 nm not intentionally doped (nid) $InAs/InAs_{0.65}Sb_{0.35}$ T2SL top contact layer (TCL), a 120 nm nid $AlAs_{0.09}Sb_{0.81}$ barrier layer (BL), a 3000 nm $InAs/InAs_{0.65}Sb_{0.35}$ T2SL absorber layer (AL) with a 5 µm targeted cut-off wavelength at 150 K, and finally a 100 nm n-doped (Te) bottom contact layer (BCL) having the same composition of the AL. The residual carrier concentration of n-type T2SL layers has been determined by capacitance-voltage measurement at 3 x $10^{15}$ $cm^{-3}$ at 150K (Zavala-Moran, 2020). The residual doping of the p-type BL layer is estimated at 1 x $10^{16}$ $cm^{-3}$.

Before the fabrication of the devices, several structural and material characterizations, such as high-resolution X-ray diffraction (HR-XRD) scan, AFM measurements, photoluminescence (PL) or time-resolved photoluminescence (TRPL), are carried out to estimate the quality of the epitaxial layers and to check the period and the targeted cut-off wavelength (Zavala-Moran, 2020). If these characterizations are suitable, with in particular minority carrier lifetime value as high as 1 µs (Bouschet, 2021), the T2SL XBn structure is processed into circular mesa photodetectors with diameters ranging from 60 to 310 µm using standard photolithography techniques, wet etching, and metal evaporation.

Single pixels were fabricated by isotropic wet chemical etching using a citric acid-based solution. After the etching step, a polymerized photoresist is deposited to protect the mesa surface from ambient air. Metal coatings are applied on both sides of detectors: Ti/Au on the TCL side and Pd/AuGeNi on the GaSb substrate.

Next, the samples were wire bonded onto a pin leadless chip carrier (LCC) and placed in the LN2-cooled JANIS cryostat ready to perform electrical and electro-optical measurements. Dark current density–voltage (J-V) measurements (under a 0-degree field of view) were performed using a KEITHLEY 6517A Electrometer to both apply the bias voltage and measure the current density delivered by the device while non-calibrated photoresponse (PR) spectra were recorded by using a Nicolet-870 Nexus Fourier transform infrared (FTIR) spectrometer with non-calibrated IR source.

## 4 CHARACTERIZATION OF THE Ga-Free BARRIER DETECTOR

Figure 8 displays the front side illuminated uncalibrated PR spectra obtained at 150 K and for different biases from -0.1V to -1V. The measurements show cut-off wavelength at 5µm, the targeted value at 150K, and quantum efficiency as high as 55% was measured elsewhere (Bouschet, 2021).

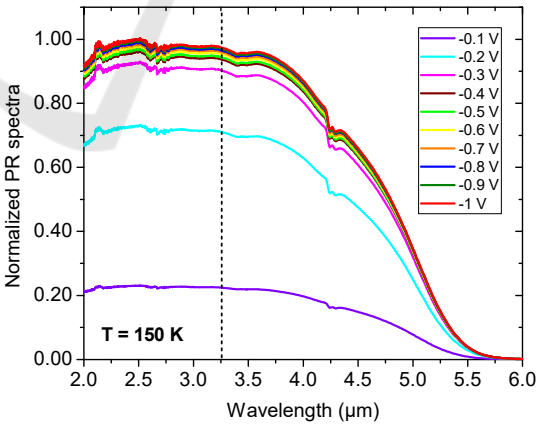


Figure 8: Normalized Photo-response spectra performed at 150 K for different biases.

At a given wavelength (λ = 3.25 µm for example), the PR increases gradually and begins to saturate at -0.4V. This non-zero operating bias value, required to fully turn on the spectral response, can be explained by the presence of a valence band offset (VBO) at

the BL-AL interface, impeding the minority carrier transport (Righer, 2019). Thus, it is necessary to apply a minimum bias of -0.40 V, the operating bias (Vop), to compensate this VBO and allow the optimal transport of holes.

T2SL is an anisotropic quantum structure in which the hole minority carriers are strongly confined in the InAsSb layer (Figure 4). This strong confinement of the carriers should generate a low value of the diffusion length and thus, penalize the PR value. To better understand the hole transport in T2SL XBn devices, especially the evolution of the diffusion length as a function of the temperature, we study the spectral PR versus voltage characteristics at different temperatures, extracted at a wavelength equal to 3.25 µm. Figure 9 shows the result obtained for 325 K (a), 170 K (b), and 90 K (c).

PR behavior seems to be temperature dependant. At 170 K, the spectral PR value (Figure 9b) appears to be saturated for higher bias than the operating bias Vop. This saturation means that the optimal transport is reached at Vop = - 400 mV with total collection of minority carriers. It is not the case at low (90 K, figure 7c) and high (325 K, figure 9a) temperature showing an unsaturated PR value with a slope for higher bias than Vop. This behavior could be linked to the diffusion length $L_D$ (eq. 2) of hole minority carriers in the T2SL device.

$$L_D = \sqrt{\frac{k_B T}{q}\,\mu_h\,\tau} \qquad (2)$$

where $k_b$ is the Boltzmann constant, $\mu_h$ the hole mobility and $\tau$ the minority carrier lifetime.

Thus, diffusion length is strongly dependant on mobility and lifetime. Optimum behavior of PR measurements is obtained at around T = 170K. At low temperature, the mobility penalizes the diffusion length (Casias, 2020) whereas it is the lifetime which reduces it at high temperature (Arounassalame, 2022).

Figure 10 shows J-V characteristics carried out for a 210 µm diameter detector in the temperature range (120 K- 270 K). At the 150 K temperature operation, dark current density as low as $3x10^{-5}$ A/cm$^2$ is recorded at operating bias V = -400mV. Such result has to be improved, since when compared to the MCT state of the art photodiode limited by diffusion dark current (Tennant, 2008), the current is 20 times higher at the corresponding cut-off wavelength. Nevertheless, this value remains in agreement with the most recent results reported on Ga-free T2SL detectors (Ting, 2018 ; Soibel, 2019 ;Wu, 2020).

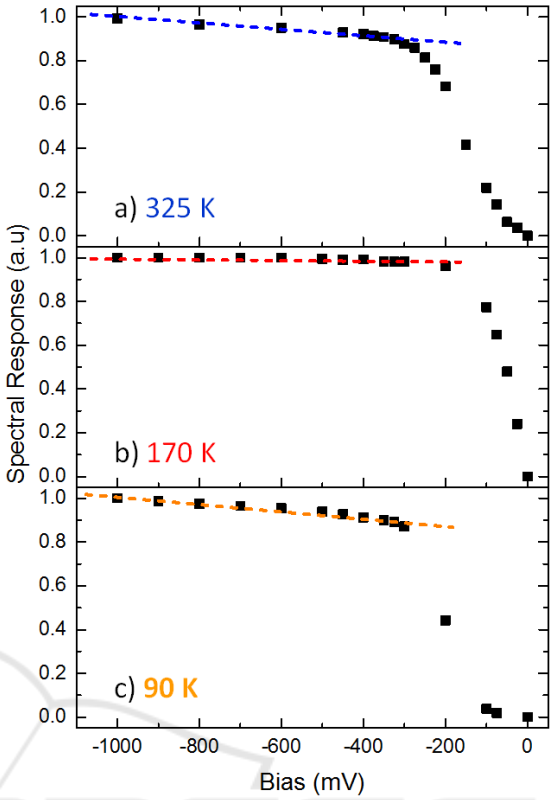


Figure 9: Uncalibrated PR recorded at 3.25µm as a function of bias at 325 K (a), 170 K (b), 90 K (c).

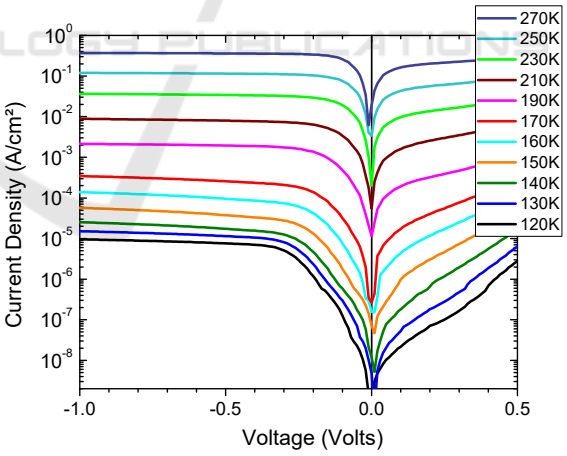


Figure 10: Dark current density characteristics of a XBn InAs/InAsSb T2SL detector at different temperatures from 120 K to 270 K.

From the dark J-V characteristics, transport regimes in the barrier detector can be identified by plotting dark current densities at Vop = - 400 mV as a function of $1/k_BT$ (Figure 11). A fit over the temperature range (150K - 270K) using the expression A exp(-$E_a$ /$k_B$ T) yields an activation

energy $E_a$ = 230meV which is approximately the T2SL energy bandgap ($E_g$) in this temperature range, signature of a diffusion limited behavior. In the temperature range (120K - 145K) the activation energy is 117 meV, approximately one half of the T2SL bandgap ($E_g$/2), indicating that the dark current is GR limited, due to the presence of a depletion region extending into the AL.

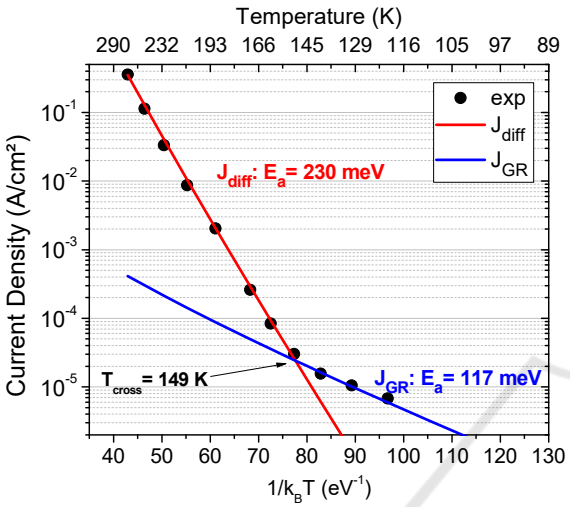


Figure 11: Arrhenius plot extracted from J-V curves in dark conditions at Vop = - 400 mV. Diffusion and Generation-Recombination dark current regimes are clearly identified.

By using residual carrier concentrations, both in the nid p-type BL (Pres) and in the nid n-type AL (Nres), extracted from capacitance-voltage (C-V) measurements (Zavala-Moran, 2020), Figure 12 shows the band diagram at V = 0 volt and T = 150 K of the considered XBn detector structure which was deduced from the experimental characterizations carried out.

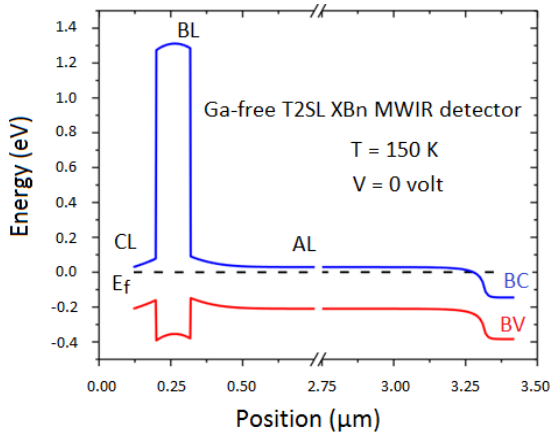


Figure 12: Calculated band diagram of the Ga-free T2SL barrier detector at 150K.

# 5 CONCLUSIONS

Ga-free InAs/InAsSb T2SL XBn MWIR photodetector has been fabricated and characterized. This detector shows cut-off wavelength at 5µm at 150K. The device highlights electrical and electro-optical performances at this temperature with dark current density values as low as $3x10^{-5}$ A/cm$^2$ in diffusion regime and an optimised photoresponse behavior. However, the operating bias equal to -400 mV remains high due to the presence of an unwanted valence band-offset at the BL-AL interface. Consequently, the AlAsSb BL has to be investigated in terms of doping, thickness layer and alloy composition to overcome this problem. It will be the subject of forthcoming studies.

# ACKNOWLEDGEMENTS

This work was partially funded by the French “Investment for the Future” program (EquipEx EXTRA, ANR 11-EQPX-0016) and by the French ANR under project HOT-MWIR (N° ANR-18-CE24-0019-01).

# REFERENCES

Arounassalame, V.; Bouschet, M.; Alchaar, R.; Ferreira, R.; Carosella, F.; Ramiandrasoa, A.; Perez, J.-P.; Péré-Laperne, N.; Christol, P.; Ribet-Mohamed, I., 2022. Anisotropic transport investigation through different etching depths in InAs/InAsSb T2SL barrier midwave infrared detector. *Infrared Physics Technology*, **126**, 104315.

Bouschet, M.; Zavala-Moran, U.; Arounassalame, V.; Alchaar, R.; Bataillon. C.; Ribet-Mohamed, I.; De Anda-Salazar, F.; Perez, J.P.; Péré-Laperne, N.; Christol, P., 2021. Influence of pixel etching on electrical and electro-optical performances of a Ga-free InAs/InAsSb T2SL barrier photodetector for mid-wave infarred imaging. *Photonics* **8**, 194.

Casias, L.K.; Morath, C.P.; Steenbergen, E.H.; Umana-Membreno, G.A.; Webster, P.T.; Logan, J.V.; Kim, J.K.; Balakrishnan, G.; Faraone, L.; Krishna, S., 2020. Vertical carrier transport in strain-balanced InAs/InAsSb type-II superlattice material. *Applied Physics Letters* **116**, 182109.

Klipstein, P., Klin, O., Grossman, S., Snapi, N., Lukomsky, I., Aronov, D., Yassen, M., Glozman, A., Fishman, T., Berkowicz, E., Magen, O., Shtrichman, I., Weiss, E., 2011. XBn barrier photodetectors based on InAsSb with high operating temperatures, *Optical Engineering,* **50**, 061002

Kroemer, H., 2004. The 6.1A family (InAs, GaSb, AlSb) and its heterostructure : a selective review, *Physica E* **20**, 196.

Lackner, D., Steger, M., Thewalt, M.L.W., Pitts, O.J., Cherng, Y.T., Watkins, S.P., Plis, E., Krishna, S., 2012. InAs/InAsSb strain balanced superlattices for optical detectors: Material properties and energy band simulations, *Journal of Applied Physics* **111**, 034507

Maimon, S., Wicks, G., 2006. nBn detector, an infrared detector with reduced dark current and higher operating temperature, *Applied Physics Letters,* **89**, 151109.

Rhiger, D.; Smith, E.P., 2019. Carrier transport in the valence band of nBn III–V superlattice infrared detectors. *Journal of Electronic Material* **48**, 6053

Soibel, A.; Ting, D.Z.; Rafol, S.B.; Fisher, A.M.; Keo, S.A.; Khoshakhlagh, A.; Gunapala, S.D., 2019. Mid-wavelength infrared InAsSb/InAs nBn detectors and FPAs with very low dark current density. *Applied Physics Letters* **114**, 161103.

Steenbergen, E.H., Cellek, O.O., Lubyshev, D., Qiu, Y., Fastenau, J.M., Liu, A.W.K., Zhang, Y.H., 2012. Study of the valence band offsets between InAs and $InAs_{1-x}Sb_x$ alloys, *Proc. SPIE* **8268**, 82680K

Tennant, W.E.; Lee, D.; Zandian, M.; Piquette, E.; Carmody, M., 2008. MBE HgCdTe technology: A very general solution to IR detection, described by "Rule 07", a very convenient heuristic. *Journal of Electronic Material*, **37**, 1406.

Ting, D.Z.; Soibel, A.; Khoshakhlagh, A.; Rafol, S.B.; Keo, S.A.; Höglund, L.; Fisher, A.M.; Luong, E.M.; Gunapala, S.D., 2018. Mid-wavelength high operating temperature barrier infrared detector and focal plane array. *Applied Physics Letters* **113**, 021101.

Webster, P. T., Riordan, N.A., Liu, S., Steenbergen, E.H., Synowicki, R.A., Zhang, Y.-H., 2015. Absorption properties of type-II InAs/InAsSb superlattices measured by spectroscopic ellipsometry, *Applied Physics Letters* **106**, 061907

Wu, D.; Li, J.; Dehzangi, A.; Razeghi, M., 2020. Mid-wavelength infrared high operating temperature pBn photodetectors based on type-II InAs/InAsSb superlattice. *AIP Advances* **10**, 025018.

Zavala-Moran, U.; Bouschet, M.; Perez, J.P.; Alchaar, R.; Bernhardt, S.; Ribet-Mohamed, I.; De Anda-Salazar, F.; Christol, P., 2020. Structural, optical and electrical characterizations of midwave infrared Ga-free Type-II InAs/InAsSb superlattice barrier photodetector. *Photonics* **7**, 76.